

Kinematic Manipulability of General Constrained Rigid Multibody Systems

John Ting-Yung Wen, *Senior Member, IEEE*, and Lee S. Wilfinger

Abstract— This paper extends the kinematic manipulability concept commonly used for serial manipulators to general constrained rigid multibody systems. Examples of such systems include multiple cooperating manipulators, multiple fingers holding a payload, multileg walking robots, and variable geometry trusses. Explicit formulas for velocity and force manipulability ellipsoids are derived and their duality explained. Singularities are classified into two types:

- 1) unmanipulable singularity;
- 2) unstable singularity.

The former is similar the singularities in serial chains where velocity manipulability ellipsoid is degenerate and force manipulability ellipsoid infinite. The latter is unique to parallel mechanisms, the velocity manipulability ellipsoid becomes infinite and force manipulability degenerate. In the case of multifinger grasp, these concepts correspond to unmanipulable or unstable grasps.

Index Terms— Kinematic stability, manipulability, multiarms, multibody systems, multifingers, parallel robots.

I. INTRODUCTION

A MECHANISM is called parallel if it consists of internal closed kinematic loops. Such mechanism has long been recognized to offer superior rigidity and load to weight ratio than their serial counterparts. A platform type of parallel mechanism was first introduced in [1] and later in [2]. This mechanism is now popularly known as Gough–Stewart platform (or simply Stewart platform). Most papers on parallel robots are based on this geometry. Extensive survey of parallel robots can be found in [3]–[5]. Most of this work is related to platform type of parallel robots, though there are later extension to truss type of robots [6], [7]. Parallel mechanism has also been introduced in machine tool design with products offered by Ingersoll, Giddings and Lewis, and Hexel. These products all consist essentially of an inverted Gough–Stewart platform, called hexapod. Other parallel machining centers have also been proposed [4], [8].

Motivated by applications to parallel robots, this paper considers the kinematic manipulability of general constrained

Manuscript received June 11, 1997; revised February 10, 1999. This paper was recommended for publication by Associate Editor H. Zhuang and Editor A. Goldenberg upon evaluation of the reviewers' comments. This work was supported in part by the Center for Automation Technologies under a Block Grant from the New York State Science and Technology Foundation.

J. T.-Y. Wen is with the Center for Automation Technologies, Department of Electrical, Computer, and Systems Engineering, Rensselaer Polytechnic Institute, Troy, NY 12180 USA (e-mail: wen@cat.rip.edu).

L. S. Wilfinger, deceased, was with the Center for Automation Technologies, Department of Electrical, Computer, and Systems Engineering, Rensselaer Polytechnic Institute, Troy, NY 12180 USA.

Publisher Item Identifier S 1042-296X(99)04979-4.

multibody systems (including passive joints and multiple closed kinematic loops). We first present a general kinematic model which considers all degrees of freedom and then imposes the constraints as algebraic conditions. Kinematic models of multifinger grasping and a 6-DOF Gough–Stewart platform are used as illustrative examples. Through the principle of virtual work, we also derive the general static force balance model which can be considered as a dual of the differential kinematics. We then extend the familiar single arm manipulability ellipsoid concept first proposed in [9]. Characterization for both velocity and force ellipsoids is presented. When applied to multiple cooperative arms employing a rigid grasp or to multiple finger grasping, this work is closely related to the work by [10] and [11] and is also closely related to the past work by [12] and [13]. We also extend the important concepts of grasp stability and manipulability. We obtain explicit characterization for both properties and present their physical interpretation. As illustrations, we include a planar Gough–Stewart platform, a full 6-DOF Gough–Stewart platform, and a planar two-finger grasping example from [12] and [13].

This paper is laid out in the following manner. We will first present the differential kinematic and static force model of a general constrained multiple-manipulator systems in Section II. The velocity and force ellipsoids, and extension of grasp stability and manipulability are presented in Section III. Section IV presents a number of examples.

Terminology and Notation: We shall use the term “spatial force” at a given frame to mean the 6×1 vector of $\begin{bmatrix} \text{torque} \\ \text{force} \end{bmatrix}$, and the term “spatial velocity” at a given frame to mean the 6×1 vector $\begin{bmatrix} \text{angular velocity} \\ \text{linear velocity} \end{bmatrix}$. Given a matrix G , we use \tilde{G} to either denote the annihilator of G ($\tilde{G}G = 0$) or the transpose of the annihilator of G^T ($G\tilde{G} = 0$). The distinction of the two cases will be clear from the context.

II. DIFFERENTIAL KINEMATICS AND STATIC FORCE MODEL

This section considers the differential kinematics and static force balance of general rigid multibody systems. Multiple-finger grasping and a Gough–Stewart platform will be used as examples.

A. Differential Kinematics

We consider a general mechanism subject to kinematic constraints. The generalized coordinate (with the constraints removed) is denoted by θ . The active joints' angles are denoted by θ_a and passive ones by θ_p . We order the angles so that

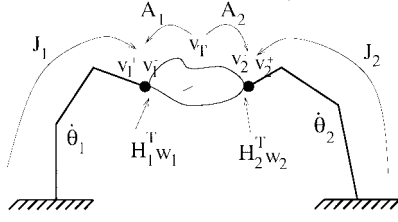


Fig. 1. Two constrained manipulators in a load-sharing configuration.

$\theta^T = [\theta_a^T, \theta_p^T]$. Consider a general constraint (written in terms of the joint velocity vector)

$$J_C(\theta)\dot{\theta} = 0. \quad (1)$$

Let the spatial velocity of the task frame be

$$v_T = J_T(\theta)\dot{\theta}. \quad (2)$$

Suppose that $J_C(\theta)$ is full rank. Then $\dot{\theta} = \tilde{J}_C \xi$, where \tilde{J}_C^T is the annihilator of J_C^T . The task velocity can be written as

$$v_T = J_T \tilde{J}_C \xi. \quad (3)$$

The mechanism is singular if $J_T \tilde{J}_C$ loses rank; in other words, there are some directions in v_T that cannot be attained (but which can be attained in other arm configurations).

1) *Multifinger Grasp Example*: As an example, consider the kinematic model of multiple fingers grasping a rigid payload shown in Fig. 1. For each serial chain, the joint velocity vector is defined as $\dot{\theta}_i$, the arm tip spatial velocity is v_i^+ , and they are related by the arm Jacobian $J_i(\theta_i)$:

$$v_i^+ = J_i(\theta_i)\dot{\theta}_i.$$

We consider a single task frame attached to the constraining rigid body (see Fig. 1) whose spatial velocity is defined as v_T . On the payload side of the contact, the spatial velocity, v_i^- , is related to the task velocity v_T by

$$v_i^- = A_i v_T \quad \text{where} \quad A_i = \begin{bmatrix} I & 0 \\ L_{it} \times & I \end{bmatrix} \quad (4)$$

where L_{it} is the vector from the i th tip to the task frame. The relative velocity at each contact is parameterized by a velocity vector W_i :

$$v_i^+ + H_i^T W_i = v_i^-$$

where the columns of H_i^T are the directions where relative velocities at the contact are allowed.

To write the multiarm kinematics more compactly, we stack all the vectors (e.g., θ_i 's are stacked into a single vector θ_a) and block diagonalize all the matrices (e.g., J_i 's form the diagonal blocks of J), except for $A^T \triangleq [A_1^T \ \dots \ A_m^T]$. Then the differential kinematic relationship can be written as

$$v^+ + H^T W = v^- \quad v^+ = J \dot{\theta}_a \quad v^- = A v_T. \quad (5)$$

Some examples of possible contacts are shown in Fig. 2.

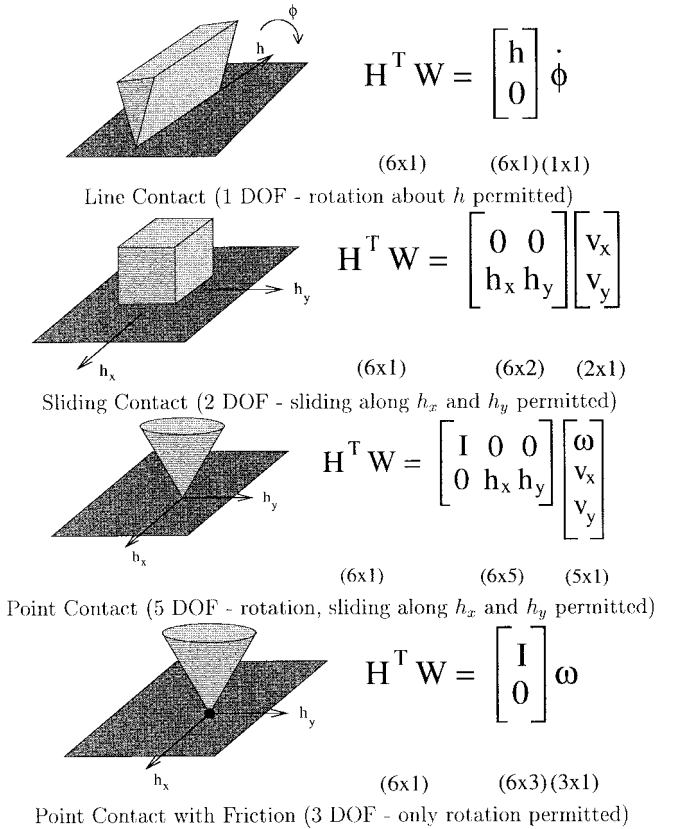


Fig. 2. Examples of different contacts.

Defining $\dot{\theta}_p = W$, we can represent the multifinger kinematic model in the general form as in (1) and (2):

$$\underbrace{\tilde{A}[J \ H^T]}_{J_C(\theta)} \begin{bmatrix} \dot{\theta}_a \\ \dot{\theta}_p \end{bmatrix} = 0 \quad (6)$$

$$\underbrace{A^+[J \ H^T]}_{J_T(\theta)} \begin{bmatrix} \dot{\theta}_a \\ \dot{\theta}_p \end{bmatrix} = v_T \quad (7)$$

where \tilde{A} is the annihilator for A and A^+ is the Moore–Penrose pseudo-inverse of A . Note that \tilde{A} is of full column rank.

It is important to note that information may be removed from J and H^T prior to calculating $J_T(\theta)$. For example, if orientation is not important for the task to be performed, it may be useful to remove the orientation components of J and H^T , and calculate a simpler form for J_T . However, the constraint Jacobian J_C should contain full information about the system.

It is also possible to include fingers having multiple (discrete) points of contact with the payload. The spatial velocities at these additional contact points can simply be added to the set of contact velocities, $\{v_i^\pm\}$. We are currently working on the extension to continuous contact, e.g., when a finger wraps around an object.

2) *Gough–Stewart Platform Example*: For another example, consider a Gough–Stewart platform which consists of two triangular plates, with spherical joints at each of their three nodes as shown in Fig. 3. Each bottom node is connected to two top nodes via a linear actuator, so there are six actuators in

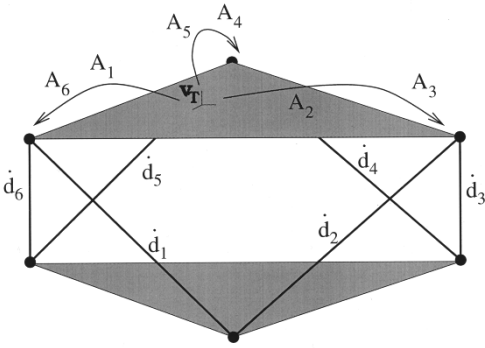


Fig. 3. Stewart platform.

all. Suppose the task frame is attached rigidly to the top plate. Let the unit vector attached to each linear actuator be denoted by e_i , where $i = 1, \dots, 6$, the length of the connection be d_i , the angular velocity of each leg be ω_i , and the angular velocity between the top plate and leg i be W_i . The rigid body transformation between the task frame and the top node connected to the i th leg is denoted by A_i [as given in (4)]. The kinematics then becomes

$$\begin{bmatrix} \omega_i \\ -d_i e_i \times \omega_i \end{bmatrix} + \begin{bmatrix} 0 \\ e_i \end{bmatrix} \dot{d}_i + \begin{bmatrix} W_i \\ 0 \end{bmatrix} = A_i v_T.$$

Define a joint velocity vector with 42 components:

$$\dot{\theta} = [\dot{d}_1 \ \dots \ \dot{d}_6 \ \omega_1 \ W_1 \ \dots \ \omega_6 \ W_6]^T. \quad (8)$$

Note that \dot{d}_1 to \dot{d}_6 are active and others are passive. Stacking all the kinematic relations up vectorially, we have

$$J\dot{\theta} = Av_T \quad (9)$$

where

$$J = \begin{bmatrix} 0 & & I & I \\ e_1 & & -d_1 e_1 \times & 0 \\ & \ddots & & \ddots \\ & & 0 & I & I \\ & & e_6 & -d_6 e_6 \times & 0 \end{bmatrix}$$

and

$$A = \begin{bmatrix} A_1 \\ \vdots \\ A_6 \end{bmatrix}. \quad (10)$$

Equation (9) can be equivalently written as

$$\begin{aligned} A^+ J \dot{\theta} &= v_T \\ \tilde{A} J \dot{\theta} &= 0. \end{aligned}$$

In addition, the legs are constrained so they cannot spin about themselves, so

$$e_i^T \omega_i = 0$$

which can also be written in terms of $\dot{\theta}$ as $J_{c1} \dot{\theta} = 0$ where J_{c1} is 6×42 . Putting the constraints together, we have J_C in (1) as

$$J_C = \begin{bmatrix} J_{c1} \\ \tilde{A} J \end{bmatrix}. \quad (11)$$

B. Force Balance

Static force balance can be considered as a dual to the kinematics. However, there is also the additional complication of static load such as gravity on each link and position feedback on the joint torque. We assume that these loads have already been excluded from the joint torque, or more specifically, we consider the joint torque τ to be the portion that balances with the load torque f_T (the force that the arm exerts at frame T). In the serial arm case, the force balance is simply $\tau = J^T(\theta) f_T$, where τ is the joint torque. This follows from the principle of virtual work:

$$\tau^T \dot{\theta} = f_T^T v_T = f_T^T J(\theta) \dot{\theta}.$$

Since this holds true for any $\dot{\theta}$, the stated force relationship follows.

In the constrained mechanism case, we can apply the principle of virtual work in a similar fashion [using the differential kinematic relationship (2) and (3) and noting that τ is now applied only at the active joints]:

$$\begin{bmatrix} \tau \\ 0 \end{bmatrix}^T \dot{\theta} = \begin{bmatrix} \tau \\ 0 \end{bmatrix}^T \tilde{J}_C \xi = f_T^T v_T = f_T^T J_T \dot{\theta} = f_T^T J_T \tilde{J}_C \xi.$$

Since this holds true for any ξ , we have the force balance equation:

$$\tilde{J}_C^T \begin{bmatrix} \tau \\ 0 \end{bmatrix} = \tilde{J}_C^T J_T^T f_T. \quad (12)$$

This can be equivalently stated as

$$\begin{bmatrix} \tau \\ 0 \end{bmatrix} = J_T^T f_T + J_C^T \eta_T \quad (13)$$

where η_T is the ‘‘internal force’’ (in the multiple-arm context, the squeeze force).

The above can be viewed from another perspective. Instead of the constraint (1), we replace it with a ‘‘virtual velocity’’ (in the same spirit as in [14] in the multiple-arm rigid grasp context):

$$v_C = J_C \dot{\theta}. \quad (14)$$

Applying the principle of virtual work again, we obtain

$$\begin{bmatrix} \tau \\ 0 \end{bmatrix}^T \dot{\theta} = f_T^T v_T + f_C^T v_C = (f_T^T J_T + f_C^T J_C) \dot{\theta} \quad (15)$$

where f_C is the force that enforces the constraint (1).

Since the explicit constraint is removed, we have

$$\begin{bmatrix} \tau \\ 0 \end{bmatrix} = J_T^T f_T + J_C^T f_C. \quad (16)$$

This shows that the internal force η_T in (13) is actually the force that enforces the constraint (1).

As an aside, it should be noted that in mechanism design, it is important to know the internal loading, f_C , for a given amount of actuator torque, τ , and task loading, f_T . This can be done unambiguously if $\mathcal{N}(J_C^T) = \{0\}$ [where $\mathcal{N}(\cdot)$ denotes the null space]. Equivalently, this means that the total number of unconstrained degrees of freedom (dimension of $\dot{\theta}$) is at least as many as the number of independent

constraints. Otherwise, one has an underdetermined problem for the constraint force. Such systems are called hyperstatic. This problem has been noted in the walking robot literature [15], [16]. In [17], several different approaches to resolve this issue have been compared.

We now apply the general frame work to the specific example of multifinger grasping. The force relationship is given by

$$\tau = J^T f \quad Hf = 0 \quad f_T = A^T f \quad (17)$$

which states that the stacked contact force f is zero in the direction where the contact is unconstrained (i.e., where relative motion is allowed) and the contact forces sum at the task frame to f_T . Solving f in terms of f_T , we have:

$$f = (A^T)^+ f_T + \tilde{A}^T f_C$$

where f_C is the force that enforces the constraint. Substituting into the τ equation and the contact constraint equation, we obtain (13):

$$\begin{bmatrix} \tau \\ 0 \end{bmatrix} = \underbrace{\begin{bmatrix} J^T \\ H \end{bmatrix}}_{J_F^T} (A^T)^+ f_T + \underbrace{\begin{bmatrix} J^T \\ H \end{bmatrix}}_{J_C^T} \tilde{A}^T f_C. \quad (18)$$

As a specific example, consider two fingers pressing against each other with a frictional point contact. In the absence of the load force, f_T , we have the force balance

$$\begin{bmatrix} \tau_1 \\ \tau_2 \\ 0 \\ 0 \end{bmatrix} = \begin{bmatrix} J_1^T \\ -J_2^T \\ [I, 0] \\ [-I, 0] \end{bmatrix} f_C.$$

The last two sets of equations mean that f_C is a pure force (no torque component). The first two equations mean that the force due to the first finger is exactly balanced with the force from the second finger.

III. VELOCITY AND FORCE MANIPULABILITY ELLIPSOIDS

A. Serial Manipulators

The velocity manipulability ellipsoid of a single, serially-linked manipulator was introduced in [9] as an indication of the relative capability of a robot arm to move in different directions. Singular value decomposition (SVD) of the Jacobian, J , is the key tool in this analysis:

$$J = U \Sigma V^T \quad (19)$$

where U and V are orthogonal matrices, and Σ consists of a diagonal matrix with rows or columns of zeros added so that its dimension is the same as that of J . The Jacobian maps a ball in the joint velocity space to an ellipsoid in the spatial task velocity space:

$$\mathcal{E}_V = \left\{ v_T: v_T = J \dot{\theta}, \|\dot{\theta}\| = 1 \right\}.$$

The principal axes of the ellipsoid are given by the columns of U (left singular vectors), u_i 's, and the lengths are given by

the singular values, σ_i 's. The right singular vectors, v_i 's, (v_i^T is the i th row of V) are the preimage of u_i 's: $Jv_i = \sigma_i u_i$. If J is less than full rank, then one or more principal axes of the ellipsoid will have zero length, and the ellipsoid will have zero volume. We say that the ellipsoid is *degenerate* in this case. If the ellipsoid is degenerate for all configurations (for example, for an arm with less than 6 DOF), then we can restrict the spatial task velocity to a lower dimensional manifold so that the ellipsoid is not degenerate at least for some configurations. If the rank of the Jacobian drops below its maximum rank at certain configurations, the arm is said to be *singular* in those configurations. With the spatial task velocity suitably restricted, singular configurations would correspond to degenerate ellipsoids. In this paper, we shall always assume that the maximum *row rank* of J over all possible configurations is full (i.e., $\mathcal{N}(J^T) = \{0\}$); this necessarily means that J is square or fat (redundant arm). Otherwise, the range of J can be suitably restricted (for all configurations) so this assumption would satisfy.

As a dual to the velocity ellipsoid, the force ellipsoid has also been introduced in the literature as the image in the end effector force space corresponding to a ball in the joint torque space:

$$\mathcal{E}_F = \{f_T: J^T f_T = \tau, \|\tau\| = 1\}.$$

By applying the SVD to J , we have $V \Sigma^T U^T f_T = \tau$. The nondegeneracy assumption means that $\Sigma^T = \begin{bmatrix} \Sigma_1 \\ 0 \end{bmatrix}$ where Σ_1 is square, diagonal, and full rank for at least some configurations. Partition $V = [V_1 \ V_2]$ with dimensions compatible with Σ_1 . Then

$$\begin{bmatrix} \Sigma_1 U^T f_T \\ 0 \end{bmatrix} = \begin{bmatrix} V_1^T \tau \\ V_2^T \tau \end{bmatrix}.$$

The bottom half of the above says that certain combination of joint torques cancel one another and does not produce an effector spatial force. They correspond to the self motion of a redundant arm. Solving the top half we obtain:

$$\mathcal{E}_F = \{f_T: f_T = U \Sigma_1^{-1} V_1^T \tau, \|\tau\| = 1\}.$$

This means that the principal axes of the force ellipsoid are the same as the velocity ellipsoid, but the lengths are the reciprocal of those in the velocity ellipsoid. When the arm is in a singular configuration, the null space of J^T would be nonzero (or one or more diagonal entries in Σ_1 are zero), implying that the force ellipsoid is infinite in the corresponding directions in U . Such configurations restrict motion but are mechanically advantageous as the mechanism can (theoretically) bear infinite load in certain direction.

In this section, we present an extension of these concepts to general constrained mechanisms. For the specific cases of multifinger grasp, the development here is similar to that in [12] and [13] and the more recent work in [18].

B. Velocity Ellipsoid

The unconstrained Jacobian, J_T , maps a unit ball in the joint velocity space to an ellipsoid in the tip contact velocity space. Due to the constraint (1), only a certain slice of the ball (resp.,

ellipsoid) is feasible. It is reasonable to define the constrained ellipsoid as the set of spatial task velocities generated by a unit ball in the *active* joint velocity space:

$$\mathcal{E}_V = \left\{ v_T: \|\dot{\theta}_a\| = 1, v_T = J_T \dot{\theta}, J_C \dot{\theta} = 0 \right\}. \quad (20)$$

The general kinematic equation (1) can be used to solve for $\dot{\theta}_p$. Partition J_C and J_T according to the dimension of θ_a and θ_p (active and passive joints):

$$J_C = [J_{C_a} \quad J_{C_p}] \quad J_T = [J_{T_a} \quad J_{T_p}]. \quad (21)$$

Typically, J_{C_p} is square, implying that the number of constraints is equal to the number passive joints. If J_{C_p} is tall, the mechanism is over-constrained meaning some of the constraints may be removed (redundant constraints) and the constraint forces cannot be uniquely solved through rigid body formulation alone. This situation sometimes occurs in walking robots [15], [16]. If J_{C_p} is fat the mechanism is under-constrained, meaning that the mechanism can always have internal motion even when all the active joints are locked.

Since the kinematic constraint always has at least one solution (otherwise the mechanism cannot move), we can write the complete solution of the passive joint velocity as

$$\dot{\theta}_p = -J_{C_p}^+ J_{C_a} \dot{\theta}_a + \tilde{J}_{C_p} \xi \quad (22)$$

where $\text{col}(\tilde{J}_{C_p})$ spans the null space of J_{C_p} , and ξ is an arbitrary vector parameterizing the null space of J_{C_p} . Substituting into (2), we have

$$v_T = (J_{T_a} - J_{T_p} J_{C_p}^+ J_{C_a}) \dot{\theta}_a + J_{T_p} \tilde{J}_{C_p} \xi. \quad (23)$$

Define the manipulability Jacobian as

$$\bar{J}_T = J_{T_a} - J_{T_p} J_{C_p}^+ J_{C_a}. \quad (24)$$

The constrained ellipsoid can be written as

$$\mathcal{E}_V = \left\{ v_T: v_T = \bar{J}_T \dot{\theta}_a, \|\dot{\theta}_a\| = 1 \right\}. \quad (25)$$

It is also straightforward to include weighted norms in the joint and/or task spaces in the above definition. Clearly, this definition makes physical sense only if $J_{T_p} \tilde{J}_{C_p} = 0$. Indeed, we consider the following classes of singularities:

- 1) *Unmanipulable Singularity*: This corresponds to configurations at which \bar{J}_T loses rank. This is the same as the singularity as in the serial manipulator case. The velocity manipulability ellipsoid becomes degenerate (one or more principal axis has zero length).
- 2) *Unstable Singularity*: This corresponds to configurations at which $J_{T_p} \tilde{J}_{C_p} \neq 0$. This type of singularity is unique to parallel mechanism and there is no counterpart in serial manipulators. The velocity manipulability ellipsoid becomes infinite in along one or more principal axis. Physically, an unstable singularity means that there exists unactuated task motion, i.e., the task frame can move even when all the active joints are locked. An example of this case is the unstable grasp in multiple-finger grasping where the payload can rotate about certain axis even when all the finger joints are locked.

It is possible that $J_{T_p} \tilde{J}_{C_p} = 0$ but $\tilde{J}_{C_p} \neq 0$. This corresponds to the existence of internal motion involving only passive joints in the mechanism that does not cause task frame motion. An example of this case is when the support legs of a Gough–Stewart platform can spin about its own axis which does not cause any platform motion. Note that even when $J_{T_p} \tilde{J}_{C_p} = 0$, \bar{J}_T may be ill-conditioned due to the $J_{C_p}^+$ term. For example, when the mechanism is near an unstable configuration, the velocity manipulability ellipsoid would be very large in certain directions.

In [19], the stable configuration condition is stated in terms of \tilde{J}_{C_a} being of full column rank [or, equivalently, $\mathcal{N}(\tilde{J}_{C_a}) = \{0\}$]. This is completely equivalent to the analysis here since $\mathcal{N}(\tilde{J}_{C_a}) = \{0\}$ if and only if $\mathcal{N}(J_{C_p}) = \{0\}$. This can be shown as follows. Let $\xi \in \mathcal{N}(\tilde{J}_{C_a})$. Then

$$0 = J_C \tilde{J}_C \xi = J_C \begin{bmatrix} \tilde{J}_{C_a} \\ \tilde{J}_{C_p} \end{bmatrix} \xi = J_{C_p} \tilde{J}_{C_p} \xi$$

which implies that $\tilde{J}_{C_p} \xi \in \mathcal{N}(J_{C_p})$. Suppose $\mathcal{N}(J_{C_p}) = \{0\}$. Then $\tilde{J}_{C_p} \xi = 0$ and therefore $J_C \xi = 0$ (since $\tilde{J}_{C_a} \xi = 0$). By construction \tilde{J}_C is of full column rank, hence, $\xi = 0$. In the reverse direction, suppose there exists $\dot{\theta}_p \in \mathcal{N}(J_{C_p})$. Then there exists ξ such that $\dot{\theta}_p = \tilde{J}_{C_p} \xi$. Now,

$$0 = [J_{C_a} \quad J_{C_p}] \begin{bmatrix} \tilde{J}_{C_a} \\ \tilde{J}_{C_p} \end{bmatrix} \xi = \begin{bmatrix} \tilde{J}_{C_a} \xi \\ 0 \end{bmatrix}.$$

Hence $\xi \in \mathcal{N}(\tilde{J}_{C_a})$.

C. Force Ellipsoid

The force ellipsoid can be intuitively defined as the set of task forces that can be applied by the mechanism with active torques (or forces) constrained on the surface of a weighted ball. We first expand the constraint force balance equation (12) as

$$\begin{aligned} J_{C_a}^T f_C + J_{C_a}^T f_T &= \tau \\ J_{C_p}^T f_C + J_{T_p}^T f_T &= 0. \end{aligned}$$

Premultiply the second equation by $\tilde{J}_{C_p}^T$, we obtain:

$$\tilde{J}_{C_p}^T J_{C_p}^T f_T = 0 \quad (26)$$

for all f_T . Clearly, if $\tilde{J}_{C_p}^T J_{C_p}^T \neq 0$ (unstable singularity), there exists some f_T that the condition cannot be satisfied. This corresponds to the task frame spatial forces that cannot be resisted by active torque and internal constraint forces alone. Hence, the mechanism is unstable. Indeed, this is precisely the condition for unstable singularities.

If the mechanism is away from the unstable singularities, there are also several cases to consider. As in the discuss of velocity manipulability, the usual case is that J_{C_p} is square (same numbers of constraints and passive joints). If J_{C_p} is tall, then not all the internal forces can be solved (the system is hyperstatic). In this case, we call this unresolvable internal force \hat{f}_c which belongs to the null space of $J_{C_p}^T$. If J_{C_p} is fat, $\tilde{J}_{C_p}^T$ is always nonzero, meaning unless $\tilde{J}_{C_p}^T J_{T_p}^T = 0$, the mechanism is at an unstable singularity.

Given the above discussion, we assume $\mathcal{N}(J_{C_p}) = \{0\}$. Then τ can be solved from (12) when the mechanism is not at an unstable singularity:

$$\tau = \left(J_{T_a}^T - J_{C_a}^T \left(J_{C_p}^T \right) + J_{T_p}^T \right) f_T = \bar{J}_T^T f_T. \quad (27)$$

We may now define the force manipulability ellipsoid as the dual of the velocity manipulability ellipsoid:

$$\mathcal{E}_F = \{f_T: \bar{J}_T^T f_T = \tau, \|\tau\| = 1\}. \quad (28)$$

As in the single arm case, we assume that $\mathcal{N}(\bar{J}_T^T) = \{0\}$ except at singular configurations (i.e., the velocity manipulability ellipsoid is not always degenerate). If this is not satisfied, we can always suitably restrict f_T (and v_T) so that it is true. The force manipulability ellipsoid has the same principal axes as the velocity manipulability ellipsoid except that their corresponding lengths are reciprocal of one another.

When the mechanism is in an unmanipulable singularity (\bar{J}_T becomes singular), the force ellipsoid becomes infinite in certain directions as in singular configurations for single arms. When the mechanism is in near an unstable singularity ($J_{T_p}, \bar{J}_{C_p} \neq 0$), \bar{J}_T^{-1} would become increasingly singular (since \bar{J}_T would be very large in certain direction). At the unstable singularity, in order for the force balance equation (12) [and hence (26)] to satisfy, f_T must be in the null space of $\bar{J}_{C_p}^T, \bar{J}_{T_p}^T$ which means that the force manipulability ellipsoid is degenerate exactly when the velocity manipulability becomes infinite.

D. Configuration Stability and Manipulability

For multifinger systems, there are two important concepts: grasp stability and grasp manipulability. A grasp is stable if any external force applied at the task frame can be resisted by suitably chosen joint torques. Equivalently, a grasp is also stable if there is no task motion independent from the joint motion. A classic example of an unstable grasp is two fingers holding a payload with frictional point contacts. The object can then spin about the line linking the contact points. Mathematically, the stable grasp condition can be stated as

$$\mathcal{N}(\tilde{H}^T A) = \{0\}$$

where H^T and A are as defined in Section II-A-1. A grasp is manipulable if any task velocity can be achieved with suitably chosen joint velocity. Mathematically, this condition can be stated as

$$\mathcal{R}(\tilde{H}^T J) \supset \mathcal{R}(\tilde{H}^T A).$$

For general mechanisms considered here, unstable grasp corresponds exactly to unstable singularity and unmanipulable grasp corresponds to unmanipulable grasp.

It is interesting to observe the dual relationship between unstable configurations and unmanipulable singular configurations. At a unmanipulable configuration, the velocity ellipsoid is degenerate (mechanism cannot move in certain directions) and the force ellipsoid is infinite (mechanism can resist infinite force in the same directions). At an unstable configuration, the force ellipsoid is degenerate (mechanism cannot resist

force in certain directions) and the velocity ellipsoid is infinite (mechanism can have any velocity using only passive joints). In a near unmanipulable configuration, large joint motion may be required to achieve small task motion. Similarly, in a near unstable configuration, large joint torques may be required to counteract small external force applied at the task frame.

E. Internal Force and Virtual Velocity

In (14), we introduced the concept of virtual velocity as the dual of the internal force. Similar to [20], we can also define a virtual velocity ellipsoid (resp. internal force ellipsoid) as the image of a unit ball of active joint velocity (resp. active joint torque) subject to the constraint that the spatial task velocity (resp. spatial task force) is zero:

$$\mathcal{E}_{V_C} = \left\{ v_C: v_C = J_C \dot{\theta}, J_T \dot{\theta} = 0, \|\dot{\theta}_a\| = 1 \right\} \quad (29)$$

$$\mathcal{E}_{F_C} = \left\{ f_C: \bar{J}_T^T J_C^T f_C = \bar{J}_T^T \begin{bmatrix} \tau \\ 0 \end{bmatrix}, \|\tau\| = 1 \right\}. \quad (30)$$

Mathematically, these ellipsoids are exactly the same as the velocity and force ellipsoids discussed before except that the subscripts T and C are exchanged. Therefore, all the preceding discussion on their computation remains valid. The concept of unstable configuration now translates to a degenerate internal force ellipsoid and infinite virtual velocity ellipsoid.

In a general mechanism, internal force may determine if a constraint can be enforced. For example, in a multifinger grasp with frictional contacts, each contact force needs to be in the friction cone to ensure that the contact can be sustained. The internal force ellipsoid provides information on the ability that the active joints may impart on the internal force. Virtual velocity provides an appealing dual to the internal force, but it is not as practically significant.

IV. ILLUSTRATIVE EXAMPLES

A. Simple Two-Arm Example

We first consider a planar two-finger grasping example. Fig. 4 shows two two-joint fingers holding a rigid object (here depicted as a bar) between them. First consider the Jacobian for each arm mapping the joint angles to the tip *translational velocity*:

$$J_i = \begin{bmatrix} -\ell_{i1}s_{i1} - \ell_{i2}s_{i12} & -\ell_{i2}s_{i12} \\ \ell_{i1}c_{i1} + \ell_{i2}c_{i12} & \ell_{i2}c_{i12} \end{bmatrix} \begin{bmatrix} \dot{\theta}_{i1} \\ \dot{\theta}_{i2} \end{bmatrix}$$

where ℓ_{ij} is the length of the j th link of the i th arm, s_{ij} is the sine of the j th angle of the i th arm, s_{ijk} is the sine of the sum of the j th and k th angles of the i th arm. The task velocity (defined as the translational velocity of a specific point on the held bar) is related to the tip velocity as:

$$v_T = v_1 + \begin{bmatrix} -L_1 s_1 \\ L_1 c_1 \end{bmatrix} \dot{\theta}_1 = v_2 + \begin{bmatrix} -L_2 s_2 \\ L_2 c_2 \end{bmatrix} \dot{\theta}_2$$

where $s_i = \sin(\theta_i)$, $c_i = \cos(\theta_i)$, and θ_i denotes the angle at the i th contact. The overall kinematics is of the following form:

$$J\dot{\theta} + H^T W = A v_T \quad (31)$$

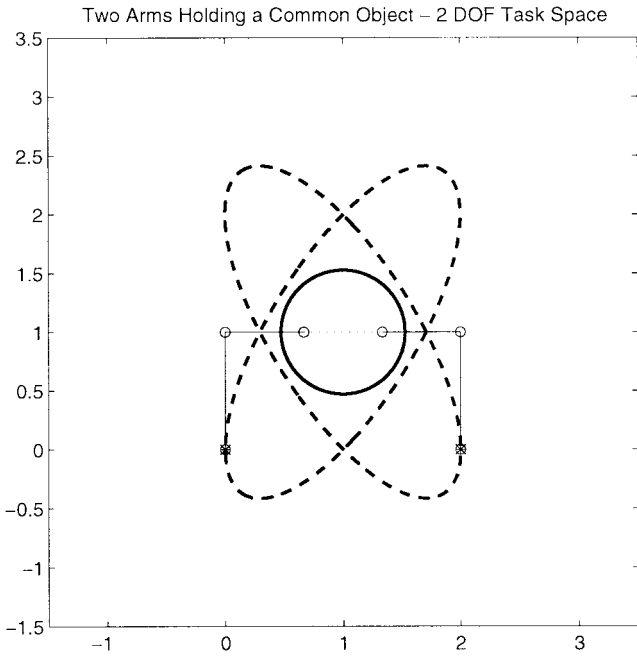


Fig. 4. Two arms holding a rigid payload.

where $J = \text{diag}\{J_1, J_2\}$, $H^T = \text{diag}\{H_1^T, H_2^T\}$, and

$$W = \begin{bmatrix} \dot{\theta}_1 \\ \dot{\theta}_2 \end{bmatrix} \quad H_i^T = \begin{bmatrix} -L_i s_i \\ L_i c_i \end{bmatrix} \quad A = \begin{bmatrix} I_{2 \times 2} \\ I_{2 \times 2} \end{bmatrix}.$$

For the constraint, the orientation needs to be included. The corresponding kinematics are:

$$J^{(c)} \dot{\theta} + H^{(c)T} W = A^{(c)} v_T \quad (32)$$

where

$$\begin{aligned} J^{(c)} &= \text{diag}\{J_1^{(c)}, J_2^{(c)}\} \\ J_i^{(c)} &= \begin{bmatrix} 1 & 1 \\ & J_i \end{bmatrix} \\ H^{(c)T} &= \text{diag}\{H_1^{(c)T}, H_2^{(c)T}\} \\ H_i^{(c)T} &= \begin{bmatrix} 1 \\ H_i^T \end{bmatrix} \\ A^{(c)} &= \begin{bmatrix} 0 & 0 \\ I_{2 \times 2} & \\ 0 & 0 \\ I_{2 \times 2} \end{bmatrix}. \end{aligned}$$

The kinematics can be written as (1) and (2) with

$$J_C = \tilde{A}^{(c)} [J^{(c)} \quad H^{(c)T}] \quad J_T = A^+ [J \quad H^T].$$

Consider in particular the configuration shown in Fig. 5. Such an example was first suggested in [20], and discussed further in [12], [13], [21], and [22]. The ellipsoid indicates that the system permits v_T in both the x and y directions. This makes sense since the robots are allowed to pivot at the contact points.

To prevent pivoting at the contact, we simply remove $H^T W$ in (31) and $H^{(c)T} W$ in (32). In this case, the ellipsoid is degenerate and the task frame can only translate in the x

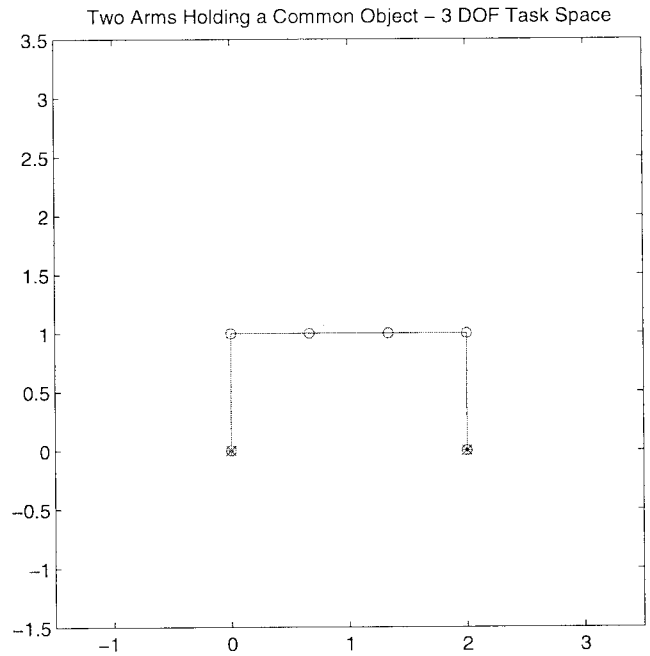


Fig. 5. Manipulability ellipsoid with orientation consideration.

direction. The degenerate ellipsoid (a horizontal line segment) is shown in Fig. 5.

In [13], this example was used to demonstrate the superiority of the ellipsoid characterization as compared to those in [20] and [23]. However, the key difference in terms of the nature of the grasp was not noted.

B. Planar Gough–Stewart Platform Example

We use a planar Gough–Stewart platform to illustrate our approach applied to a mechanism that is *not* a single closed chain. Fig. 6 shows various different planar Gough–Stewart platforms each with 3 active prismatic joints and 6 passive rotational joints.

We consider the task velocity as the linear velocity of the center of the platform.

$$A v_T = J \dot{d} + H^T W \quad (33)$$

where $J = \text{diag}\{J_1, J_2, J_3\}$, $H^T = \text{diag}\{H_1^T, H_2^T, H_3^T\}$, $d = [d_1, d_2, d_3]^T$ (prismatic joint velocities), $W = [W_1, W_2, W_3]^T$, $A = [I_{2 \times 2} \quad I_{2 \times 2} \quad I_{2 \times 2}]^T$

$$\begin{aligned} J_i &= \begin{bmatrix} c_i \\ s_i \end{bmatrix} \\ W_i &= \begin{bmatrix} \dot{\theta}_i \\ \dot{\phi}_i \end{bmatrix}. \end{aligned}$$

θ_i is the angular velocity of leg i with respect to the ground, ϕ_i is the angular velocity of the platform with respect to leg i , $c_i \triangleq \cos(\theta_i)$, $s_i \triangleq \sin(\theta_i)$.

As in the previous example, the constraint kinematics include orientation and therefore needs to be separately stated:

$$A^{(c)} v_T = J^{(c)} \dot{d} + H^{(c)T} W \quad (34)$$

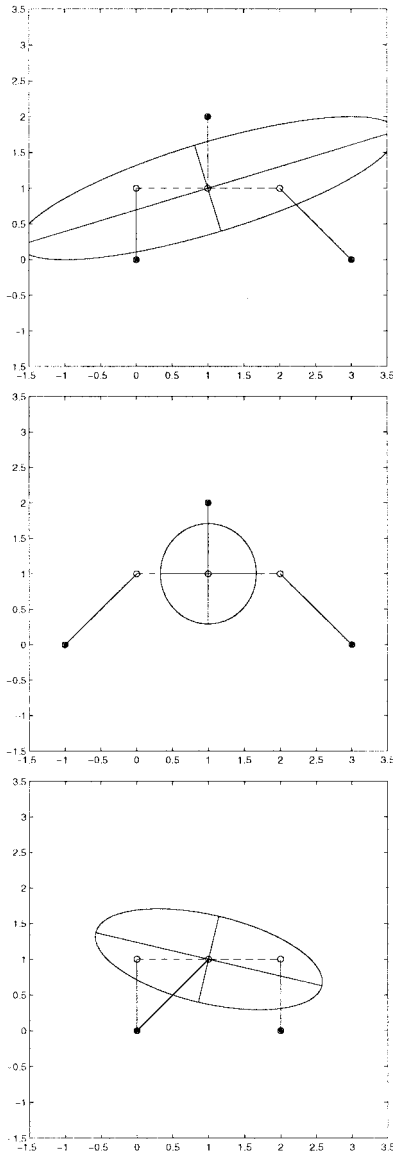


Fig. 6. Velocity ellipsoids for various Gough–Stewart platforms.

where $J^{(c)} = \text{diag}\{J_1^{(c)}, J_2^{(c)}, J_3^{(c)}\}$, $H^{(c)T} = \text{diag}\{H_1^{(c)T}, H_2^{(c)T}, H_3^{(c)T}\}$, $A^{(c)T} = [A_1^{(c)T}, A_2^{(c)T}, A_3^{(c)T}]$ and

$$\begin{aligned} J_i^{(c)} &= \begin{bmatrix} 0 \\ J_i \end{bmatrix} \\ H_i^{(c)T} &= \begin{bmatrix} [1, 1] \\ H_i \end{bmatrix} \\ A_i^{(c)} &= \begin{bmatrix} [0, 0] \\ I_{2 \times 2} \end{bmatrix}. \end{aligned}$$

Transforming these equations to the form that we have used, (1) and (2), we have

$$J_C = \tilde{A}^{(c)} [J^{(c)} \quad H^{(c)T}] \quad (35)$$

$$J_T = A^+ [J \quad H^T]. \quad (36)$$

Using the results presented earlier, ellipsoids for different configurations can be readily generated (as shown in Fig. 6).

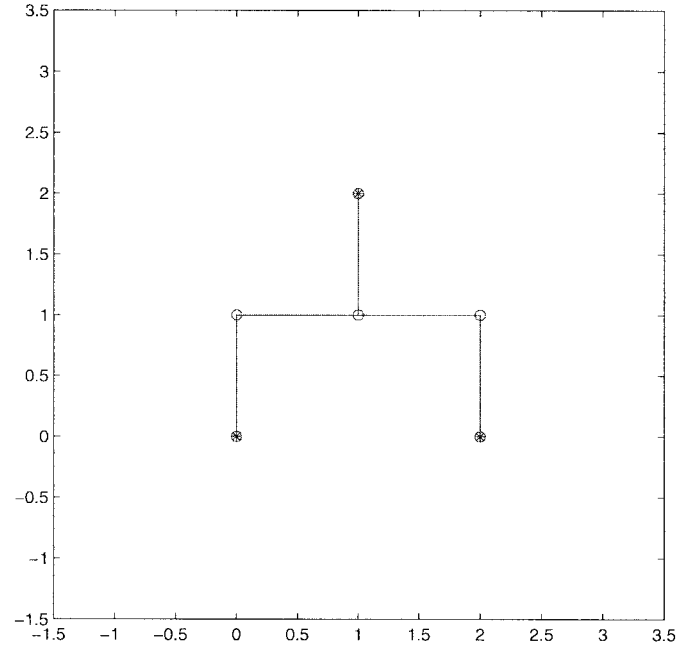


Fig. 7. Unstable configuration.

All of these cases correspond to stable, nonsingular configurations.

For the configuration shown in Fig. 7, $\mathcal{N}\{\tilde{J}_{C_a}\} \neq \{0\}$. For the case shown, the mechanism can have a pure horizontal motion involving only the passive joints ($\dot{\theta}_1 = \dot{\theta}_2 = -\dot{\theta}_3 = 1$). From a force perspective, the unstable configuration means that the mechanism cannot resist x direction force applied at the task frame.

When the mechanism is near an unstable configuration, it may not be unstable mathematically, but the ellipsoid will be badly conditioned. As shown in Fig. 8, the motion in the x direction is much larger than in the y direction. When the mechanism moves in to the unstable configuration, the ellipsoid becomes infinite in the x direction. From the force perspective, this suggests that a nearly unstable configuration is also highly undesirable as large forces from the active joints are needed to counteract disturbance force at the task frame. We have constructed a physical 3-DOF Gough–Stewart platform, and have indeed verified that unstable and nearly unstable configurations can have large internal motion with all the active joints locked. When the ellipsoid is well conditioned, such internal motion is no longer possible.

C. Six-DOF Gough–Stewart Platform Example

We now consider a 6-DOF Gough–Stewart platform. Let the three base nodes be at

$$x_1 = \begin{bmatrix} -1 \\ -1 \\ 0 \end{bmatrix} \quad x_2 = \begin{bmatrix} 1 \\ -1 \\ 0 \end{bmatrix} \quad x_3 = \begin{bmatrix} 0 \\ 1 \\ 0 \end{bmatrix}.$$

The top platform is an isosceles triangle with the two equal sides of length 1.12 and the third side of length 1. The task velocity, v_T , is defined as the translational velocity of the half way point of the line perpendicular to the base of the isosceles

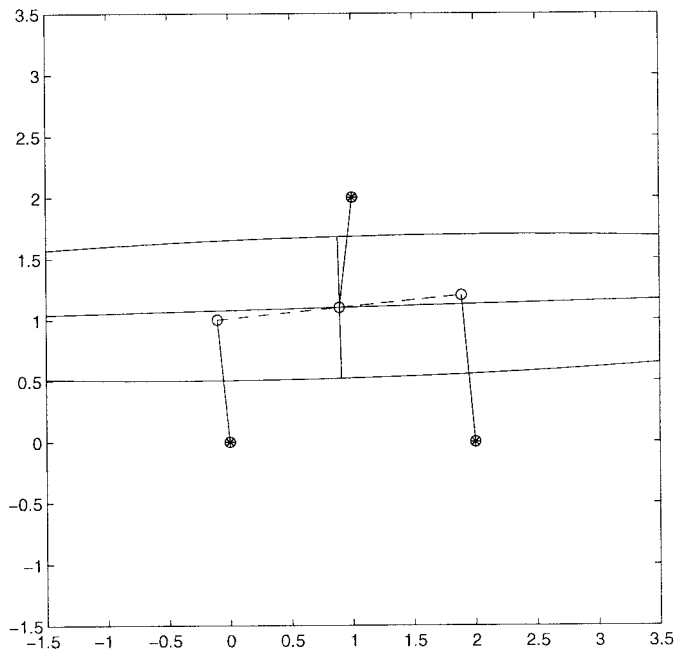


Fig. 8. Nearly unstable configuration.

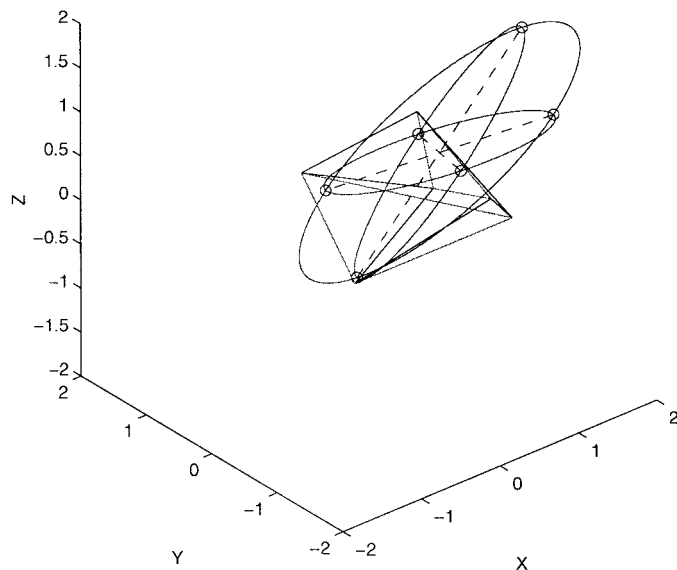


Fig. 10. Three-dimensional ellipsoid for six-DOF Gough-Stewart platforms: case 2.

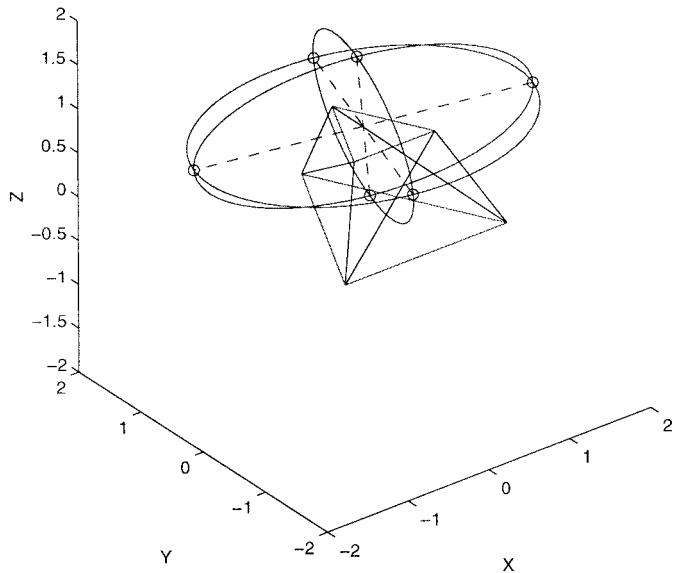


Fig. 9. Three-dimensional ellipsoid for six-DOF Gough-Stewart platforms: case 1.

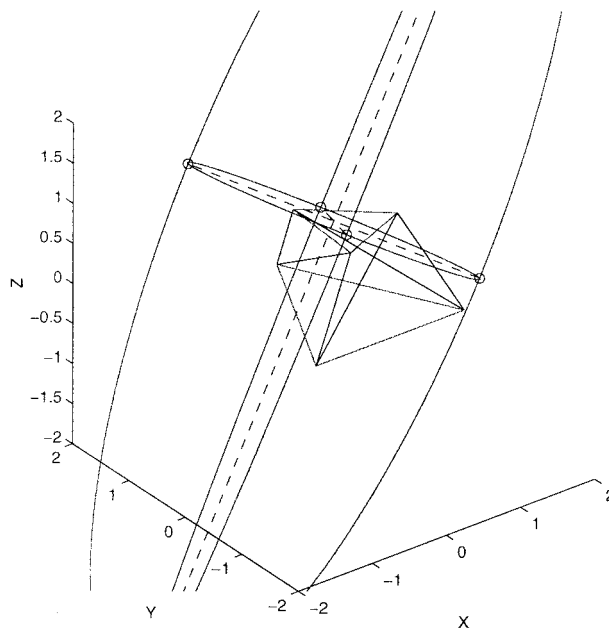


Fig. 11. Three-dimensional ellipsoid for 6-DOF Gough-Stewart platforms: case 3.

platform. As in the two previous examples, the task velocity only involves the linear motion but the constraints need to include orientation. Therefore, the kinematics developed in Section II-A needs to be slightly modified. With $\dot{\theta}$ as defined in (8), the task velocity kinematics is now

$$\begin{bmatrix} e_1 & & -d_1 e_1 \times & 0_{3 \times 3} & & \\ & \ddots & & & \ddots & \\ & & e_6 & & & -d_6 e_6 \times & 0_{3 \times 3} \end{bmatrix} \dot{\theta} = \begin{bmatrix} I_{3 \times 3} \\ \vdots \\ I_{3 \times 3} \end{bmatrix} v_T. \tag{37}$$

The constraint equation, (1), is the same as in Section II-A, given by (11).

The velocity ellipsoids of the Gough-Stewart platform in three different configurations are shown in Figs. 9–11 (the force ellipsoids have the same principal axes but reciprocal length). In the first case, the platform is horizontal. In the second case, the task frame is rotated 45° about the axis $[0.71 \ 0.71 \ 0]^T$. In the third case, the task frame is rotated 22.5° about the vertical axis $[0 \ 0 \ 1]$.

In each case, three ellipses lying in the plane generated by two of the principal axes are shown. In the first case, the ellipse is well conditioned with the lengths of principal axes:

{1.78, 1.43, 0.81}. In the second case, the ellipsoid becomes less well conditioned, the lengths of the principal axes are {2.31, 1.62, 0.29}. The motion parallel to the platform is more difficult than other directions. In the third case, the lengths of the principal axes are {5.62, 1.69, 1.49}. Even though the ellipsoid is fairly well conditioned (condition number of the singular values is 3.78), but external forces along the principal axis that corresponds to 5.62, $[-0.54 \ 0.12 \ -0.83]$, cannot be resisted as easily as in other directions.

V. CONCLUSION

This paper generalizes the velocity and force manipulability to general constrained multibody systems. Such systems include simple closed kinematic chain as two arms jointly holding a payload, multiple kinematic chains as in multi-finger grasping, and more complex structures as multiple Gough–Stewart platforms. We classify singularities into two classes: unmanipulable singularities and unstable singularities. For the former, velocity ellipsoid is degenerate and force ellipsoid infinite. For the latter, velocity ellipsoid is infinite and force ellipsoid degenerate. In general, unstable (or nearly unstable) configurations need to be carefully considered in the kinematic analysis, otherwise there may be uncontrolled motion or large joint loading. Future work will include optimal kinematic synthesis based on the manipulability ellipsoids and consideration of systematic addition of kinematic constraints or actuation to modify the singularity structure.

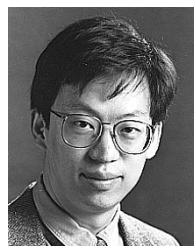
ACKNOWLEDGMENT

The authors would like to thank Dr. C. Park for his helpful discussions. The work described in this paper was based on the late L. S. Wilfinger's doctoral research. He was involved in a tragic accident in May 1997 and passed away in August 1997. This paper is dedicated to his memory.

REFERENCES

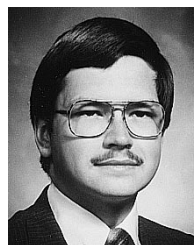
- [1] V. E. Gough, "Contribution to discussion to papers on research in automobile stability on control and in tyre performance," in *Proc. Automotive Division Instrum. Eng.*, 1956.
- [2] D. Stewart, "A platform with 6 degrees of freedom," in *Proc. Inst. Mech. Eng.*, 1965, vol. 180, pts. 1 and 15, pp. 371–386.
- [3] J.-P. Merlet, "Parallel manipulators: State of the art and perspective," in *Robotics, Mechatronics and Manufacturing Systems*, T. Takamori and K. Tsuchiya, Eds. New York: Elsevier, 1993.
- [4] B. S. Stevens and R. Clavel, "The delta parallel robot, its future in industry," in *Proc. ISRAM*, Aug. 1994, pp. 273–278.
- [5] M. Uchiyama, "Structures and characteristics of parallel manipulators," *Adv. Robot.*, vol. 8, no. 6, pp. 545–557, Dec. 1994.
- [6] M. Tanaka, "Motion/configuration control of a truss-type parallel manipulator with redundancy," in *Proc. Jpn.–U.S. Symp. Flexible Automat.*, Kyoto, Japan, Mar. 1990.
- [7] G. J. Hamlin and A. C. Sanderson, "TETRABOT: A modular approach to parallel robotics," *IEEE Robot. Automat. Mag.*, vol. 4, no. 1, Mar. 1997.
- [8] S. J. Ryu, C. Park, J. Kim, J. Hwang, J. Kim, and F. C. Park, "Design and performance analysis of a parallel mechanism-based universal machining center," Tech. Rep., Seoul Nat. Univ., Seoul, Korea, 1998.
- [9] T. Yoshikawa, "Manipulability of robotic mechanisms," *Int. J. Robot. Res.*, vol. 4, no. 2, pp. 3–9, 1985.
- [10] F. C. Park and J. W. Kim, "Manipulability and singularity analysis of multiple robot systems: A geometric approach," in *Proc. 1998 IEEE Int. Conf. Robot. Automat.*, Leuven, Belgium, May 1998, pp. 1032–1037.

- [11] A. Bicchi and D. Prattichizzo, "Manipulability of cooperating robots with passive joints," in *Proc. 1998 IEEE Int. Conf. Robot. Automat.*, Leuven, Belgium, May 1998, pp. 1038–1044.
- [12] P. Chiacchio, S. Chiaverini, L. Sciavicco, and B. Siciliano, "Reply to 'comments on' global task space manipulability ellipsoids for multiple-arm systems' and further considerations," *IEEE Trans. Robot. Automat.*, vol. 9, pp. 235–236, Apr. 1993.
- [13] A. Bicchi, C. Melchiorri, and D. Balluchi, "On the mobility and manipulability of general multiple limb robots," *IEEE Trans. Robot. Automat.*, vol. 11, pp. 215–228, Apr. 1995.
- [14] M. Uchiyama and P. Dauchez, "Symmetric kinematic formulation and nonmaster/slave coordinated control of two-arm robots," *Adv. Robot.: Int. J. Robot. Soc. Jpn.*, vol. 7, no. 4, pp. 361–383, 1993.
- [15] V. R. Kumar and K. J. Waldron, "Force distribution in closed kinematic chains," *IEEE J. Robot. Automat.*, vol. 4, pp. 657–664, Dec. 1988.
- [16] C. A. Klein and S. Kittivacharapong, "Optimal force distribution for the legs of a walking machine with friction cone constraints," *IEEE Trans. Robot. Automat.*, vol. 6, pp. 73–85, Feb. 1990.
- [17] M. Nahon, "A comparison of methods for the control of redundantly-actuated robotic systems," *J. Intell. Robot. Syst.*, vol. 14, pp. 3–20, 1995.
- [18] F. Park, "Manipulability of closed kinematic chains," *ASME J. Mech. Design*, 1997.
- [19] J. T. Wen and L. S. Wilfinger, "Kinematic manipulability of general constrained rigid multibody systems," in *Proc. 1998 IEEE Int. Conf. Robot. Automat.*, Leuven, Belgium, May 1998, pp. 1020–1025.
- [20] P. Chiacchio, S. Chiaverini, L. Sciavicco, and B. Siciliano, "Global task space manipulability ellipsoids for multiple-arm systems," *IEEE Trans. Robot. Automat.*, vol. 7, no. 5, pp. 678–685, Oct. 1991.
- [21] C. Melchiorri, "Comments on 'global task space manipulability ellipsoids for multiple-arm systems' and further considerations," *IEEE Trans. Robot. Automat.*, vol. 9, pp. 232–235, Apr. 1993.
- [22] A. Bicchi and C. Melchiorri, "Manipulability measures of cooperating arms," in *Proc. 1993 Amer. Contr. Conf.*, San Francisco, CA, June 1993, pp. 321–325.
- [23] S. Lee, "Dual redundant arm configuration optimization with task-oriented dual arm manipulability," *IEEE Trans. Robot. Automat.*, vol. 5, pp. 78–97, Feb. 1989.



John Ting-Yung Wen (SM'93) received the B.Eng. degree from McGill University, Montreal, P.Q., Canada, in 1979, the M.S. degree from the University of Illinois, Urbana, in 1981, and the Ph.D. degree from Rensselaer Polytechnic Institute (RPI), Troy, NY, in 1985, all in electrical engineering.

From 1981 to 1983, he was a System Engineer at Fisher Control Company, Marshalltown, IA, where he worked on the coordination control of a pulp and paper plant. From 1985 to 1988, he was a Member of Technical Staff at the Jet Propulsion Laboratory, Pasadena, CA, where he worked on the modeling and control of large flexible structures and multiple-robot coordination. Since 1988, he has been with the Department of Electrical, Computer, and Systems Engineering, RPI, where he is currently a Professor. He is also a member of the New York Center for Automation Technologies. His current research interests are in the area of modeling and control of multibody mechanical systems, distributed motion and process control, and robotics for surgical applications.



Lee S. Wilfinger received the B.S. degree in electrical and computer engineering from Carnegie Mellon University, Pittsburgh, PA, in 1989 and the M.S. degree in computer and systems engineering from Rensselaer Polytechnic Institute, Troy, NY, in 1992.

His research was in the areas of force control and control of multiple robot arms.